ACCOUNTS
of chemical research

Screw Dislocation Driven Growth of Nanomaterials

FEI MENG, STEPHEN A. MORIN,‡ AUDREY FORTICAUX, AND SONG JIN*

Department of Chemistry, University of Wisconsin—Madison, 1101 University Avenue, Madison, Wisconsin 53706, United States

RECEIVED ON JANUARY 4, 2013

CONSPECTUS

Nanoscience and nanotechnology impact our lives in many ways, from electronic and photonic devices to biosensors. They also hold the promise of tackling the renewable energy challenges facing us. However, one limiting scientific challenge is the effective and efficient bottom-up synthesis of nanomaterials. We can approach this core challenge in nanoscience and nanotechnology from two perspectives: (a) how to controllably grow high-quality nanomaterials with desired dimensions, morphologies, and material compositions and (b) how to produce them in a large quantity at reasonable cost. Because many chemical and physical properties of nanomaterials are size- and shape-dependent, rational syntheses of nanomaterials to achieve desirable dimensionalities and morphologies are essential to exploit their utilities. In this Account, we show that the dislocation-driven growth mechanism, where screw dislocation defects provide self-perpetuating growth steps to enable the anisotropic growth of various nanomaterials at low supersaturation, can be a powerful and versatile synthetic method for a wide variety of nanomaterials.

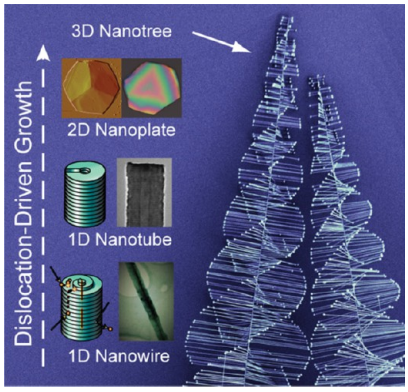

Despite significant progress in the last two decades, nanomaterial synthesis has often remained an "art", and except for a few well-studied model systems, the growth mechanisms of many anisotropic nanostructures remain poorly understood. We strive to go beyond the empirical science ("cook-and-look") and adopt a fundamental and mechanistic perspective to the anisotropic growth of nanomaterials by first understanding the kinetics of the crystal growth process. Since most functional nanomaterials are in single-crystal form, insights from the classical crystal growth theories are crucial. We pay attention to how screw dislocations impact the growth kinetics along different crystallographic directions and how the strain energy of defected crystals influences their equilibrium shapes. Furthermore, such inquiries are supported by detailed structural investigation to identify the evidence of dislocations. The dislocation-driven growth mechanism not only can unify the various explanations behind a wide variety of exotic nanoscale morphologies but also allows the rational design of catalyst-free solution-phase syntheses that could enable the scalable and low cost production of nanomaterials necessary for large scale applications, such as solar and thermoelectric energy conversions, energy storage, and nanocomposites.

In this Account, we discuss the fundamental theories of the screw dislocation driven growth of various nanostructures including one-dimensional nanowires and nanotubes, two-dimensional nanoplates, and three-dimensional hierarchical tree-like nanostructures. We then introduce the transmission electron microscopy (TEM) techniques to structurally characterize the dislocation-driven nanomaterials for future searching and identifying purposes. We summarize the guidelines for rationally designing the dislocation-driven growth and discuss specific examples to illustrate how to implement the guidelines. By highlighting our recent discoveries in the last five years, we show that dislocation growth is a general and versatile mechanism that can be used to grow a variety of nanomaterials via distinct reaction chemistry and synthetic methods. These discoveries are complemented by selected examples of anisotropic crystal growth from other researchers. The fundamental investigation and development of dislocation-driven growth of nanomaterials will create a new dimension to the rational design and synthesis of increasingly complex nanomaterials.

Introduction

Synthesizing nanoscale building blocks of arbitrary dimensions, morphologies, and materials from bottom-up has been a major pursuit in nanoscience and nanotechnology. Anisotropic nanostructures, such as one-dimensional (1D) nanowires (NWs), nanorods (NRs), and nanotubes (NTs), two-dimensional (2D) nanoplates, and three-dimensional (3D) hierarchical structures have exhibited new fundamental

Published on the Web 06/05/2013 www.pubs.acs.org/accounts
10.1021/ar400003q

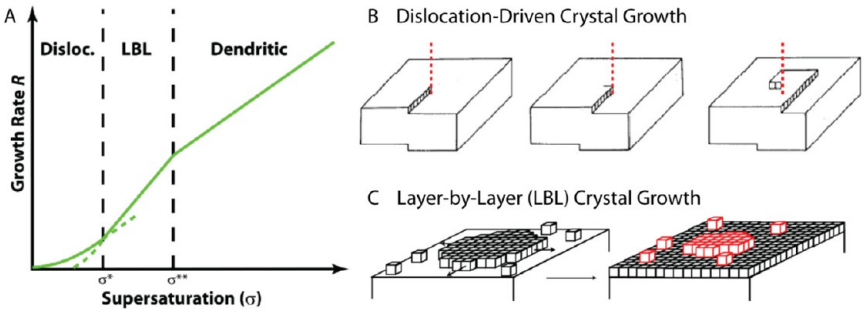

FIGURE 1. Supersaturation and crystal growth. Schematic illustrations for (A) growth rate of different crystal growth modes as a function of supersaturation,[14] (B) propagation of screw dislocation growth spirals, and (C) nucleation and expansion of 2D nuclei in LBL growth.[15] Panel A adapted from ref 14. Reprinted with permission from AAAS.

physical properties and demonstrated promising utility in nanoelectronics, nanophotonics, solar energy conversion, thermoelectric and electrochemical energy storage, and chemical and biological sensing.[1−6] It is important to understand the fundamental anisotropic growth process of nanomaterials so that rational and controllable syntheses can be designed accordingly to prepare nanostructures suited toward specific applications.

Since most functional nanostructures are single crystals, their formation process is essentially the process of crystal growth. Therefore, the challenge to grow anisotropic nanostructures is to break the symmetry in crystal growth to promote the formation of highly anisotropic crystals instead of polyhedral crystals or thin films. In contemporary literature, catalysts or templates are widely adopted approaches to regulate the crystal growth to yield anisotropic nanostructures.[1] For example, in the catalyst-driven growth of 1D nanostructures, such as vapor−liquid−solid (VLS),[7,8] solution−liquid−solid,[9] and vapor−solid−solid[10] mechanisms, the presence of catalyst particles promotes crystal growth through the catalyst−NW interface over the NW sidewall surface, and the structure can thus propagate anisotropically. Templates can physically inhibit or suppress the growth along a certain direction and result in anisotropic structures.[1]

Here we discuss the screw dislocation driven growth mechanism of anisotropic nanomaterials, in which screw dislocations, common defects in crystals, provide self-perpetuating growth steps and break the symmetry of crystal growth. No catalyst or template is required because the anisotropy is due to the growth kinetic differences along different crystallographic directions caused by the dislocations.[11−14] We show that the growth of a variety of nanostructures, from 1D NWs and NTs to 2D nanoplates and 3D nanostructures with different compositions can be explained by the dislocation-driven mechanism. Practical techniques to characterize dislocation-driven nanomaterials to confirm their growth mechanism are then introduced to facilitate the search of these materials. We also outline a general framework to design rational dislocation-driven nanomaterial growth and review a wide variety of materials synthesized using both vapor and solution growth methods following this guideline, demonstrating the generality of the dislocation-driven mechanism.

Classical Crystal Growth Theories

Since the key to anisotropic crystal growth is controlling and differentiating the kinetics of crystal growth along specific directions to break the symmetry of crystal growth, we first review the fundamental crystal growth processes.[15] According to the classical crystal growth theory, the supersaturation (σ) of the system is the driving force for crystal growth:[15]

$$\sigma = \ln(c/c_0)$$

where c is the precursor concentration and c_0 is the equilibrium concentration. The dislocation-driven growth, layer-by-layer (LBL) growth, and dendritic growth modes progressively dominate the crystal growth as supersaturation increases (Figure 1A).

The screw dislocation defects can promote bulk crystal growth at low supersaturation conditions. The line of a screw dislocation creates step edges upon intersection with a crystal surface, which will propagate as self-perpetuating growth spirals (Figure 1B).[16] Thus there are always step edges to which atoms can be added, and there is no need to overcome the energy barrier to nucleate new crystal steps; therefore the crystal growth can proceed under low supersaturation conditions. This model, known as the Burton−Cabrera−Frank (BCF) theory,[17,18] predicts a dislocation growth rate linearly dependent on supersaturation and dominant over other crystal growth modes below a critical supersaturation (σ^*). This growth kinetic is a characteristic feature of dislocation-driven growth that can distinguish it from other growth modes.

Under intermediate supersaturation conditions, the LBL mode starts to take over the crystal growth. Here, the nucleation of successive crystal layers is necessary to create the new step edges that facilitate the addition of more atoms on crystal facets (Figure 1C). Therefore a higher supersaturation is necessary to overcome the energy barrier needed for nucleating new steps, which results in the kinetics of the LBL growth rate exponentially dependent on supersaturation.

At high supersaturation (above σ^{**}, Figure 1a), crystal growth is dominated by the dendritic mode. In this growth regime, the precursor flux at the crystal surface is so high that nonequilibrium monomer aggregation occurs and the rate of diffusion from the surrounding environment toward the crystal surface limits the rate of crystal growth; therefore this mode is also referred to as diffusion-limited aggregation (DLA). Furthermore, at kinks or corners of the crystal, the concentration gradient between the high-supersaturation reaction media and the crystal surface is the highest; thus the growth rate is the fastest, which usually yields crystals with rough surfaces and fractal patterns, such as snowflakes.[19]

We emphasize that these crystal growth theories are generally applicable regardless of the reaction media (vapor, solution, or melt) or their outcomes (bulk single crystals, thin films, or nanostructures). These theories on crystal growth kinetics are the basis for manipulating the growth rates along different crystal directions to enable anisotropic nanomaterial growth. Just as understanding and controlling reaction kinetics in organic synthesis is the key to synthesizing diverse and complex molecules, adding the kinetic perspective to nanomaterial growth will enable the rational design of complex nanomaterial synthesis. Note that VLS and analogous catalyst-driven NW growth only rely on the LBL crystal growth, but the differential kinetics of LBL growth through the catalyst–NW interface and the vapor–solid interface enables anisotropic crystal growth.

Dislocation-Driven Growth of Nanomaterials: Morphological Variations

Using preferred dislocation-driven growth under low supersaturation conditions, we can explain a variety of distinct morphologies, including 1D NW and NT, 2D nanoplate, and 3D hyperbranching nanostructure (Figure 2). The key is the difference in the step growth rates between different growth fronts, for example, the velocity of steps at the dislocation core (v_c) and those at the outer edges (v_o), which leads to different dimensionalities. Moreover, the strain and stress caused by dislocation defects also impact nanomaterial

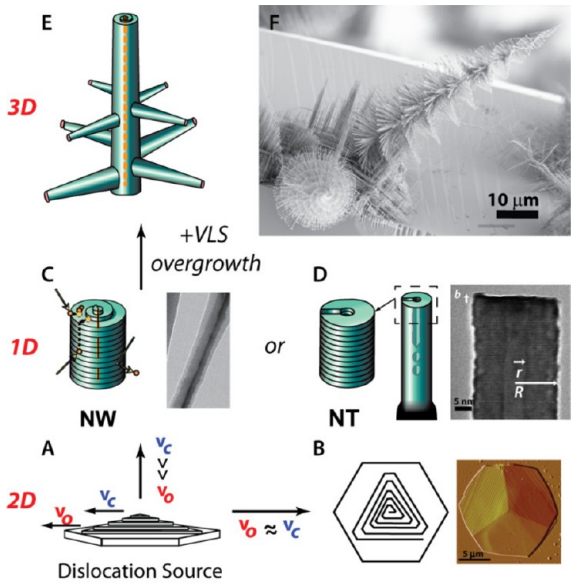

FIGURE 2. Formation pathways for different nanostructures driven by screw dislocations.

morphologies, which can also be recognized as signatures of dislocation-driven growth.

2D Nanoplates. Starting from a screw dislocation hillock on the surface (Figure 2A), it is intuitive to explain the formation of 2D nanoplates by BCF theory. The key is to pay attention to the crystal growth step velocities at different positions from the dislocation core.[20] When v_o is equal to v_c, the newly generated steps near the dislocation core propagate at the same rate with earlier steps at the outer edge of the growth spiral; thus the dislocation hillock spreads in 2D fashion without a step pile up (Figure 2B). This is the most typical process during bulk crystal growth when dislocation-driven growth is in operation and does not intrinsically lead to highly anisotropic crystals. However, when the supersaturation is low, the slope of dislocation hillocks will be small, which leads to the formation of highly squashed pyramids that can be approximated as nanoplates.[20]

1D Nanowire and Eshelby Twist. If and when v_o is impeded due to impurities, mass transport, size of the dislocated seeding crystals, or other factors that remain to be understood,[21] the newly generated spiral steps will catch up, resulting in step bunching and formation of cylinders. When this occurs, highly anisotropic 1D crystal growth (Figure 2C) is enabled under low supersaturation because axial growth on dislocation spiral steps is preferred while energetically unfavorable creation of 2D nuclei on the sidewall is required for LBL growth along the radial direction where no dislocation is present. As a consequence, the crystal can rapidly propagate along the line direction of the dislocation to

form a NW. At slightly higher supersaturation, LBL growth on the sidewall can proceed at moderate rate but still slower than dislocation-driven growth, which leads to decreased aspect ratio and produces NRs often with tapering diameters.

The presence of a screw dislocation disrupts the perfect periodicity of the crystal. A strain field is thereby generated, forcing the 1D crystal to twist about its axial axis,[16,22] which is known as the "Eshelby twist". The strain energy associated with screw dislocations per unit length (E) is quadratically dependent on the magnitude of the Burgers vector (**b**) of the screw dislocation:

$$E = \frac{\mathbf{b}^2\mu}{4\pi}\int_{r_0}^{R}\frac{dr}{r} = \frac{\mathbf{b}^2\mu}{4\pi}\ln\left(\frac{R}{r_0}\right)$$

where μ is the shear modulus, R is the radius of the cylinder containing the dislocation, and r_0 is the core radius of the dislocation. The Eshelby twist, α (in radians per unit length), is predicted as[16,22]

$$\alpha = \frac{\mathbf{b}}{\pi R^2}$$

The effect of the Eshelby twist in bulk crystals and micrometer-sized whiskers is rather minute due to their large size.[16] In nanowires, the Eshelby twist is more pronounced due to the $1/R^2$ dependence. Particularly in branched nanostructures, the periodically rotating branches (Figure 2F) reveal the twist in the central NW, enabling direct measurement of lattice twist and a simple estimate of the magnitude of **b**.[23] We note that although the analytical expression of Eshelby twist was derived using continuum elasticity theory, it is still applicable to nanoscale structures. More detailed atomistic representation of the Eshelby twist based on molecular dynamics was recently made for thin NWs and NTs.[24−26]

1D Nanotube. The formation of single-crystal NTs can be a signature of the nanomaterial growth driven by dislocations with large magnitude of Burgers vector **b** (Figure 2D). With increasing **b**, the strain energy within the crystal will eventually exceed the surface energy required for creating a new inner surface and cause the dislocation core to become hollow.[14,27] In a bulk crystal or thin film, the radius (r) of the hollow channel is directly dependent on the magnitude of the Burgers vector (**b**):[27]

$$r = \frac{\mu\mathbf{b}^2}{8\pi^2\gamma}$$

where γ is the surface energy. This mechanism causes the frequently observed micropipe structures in dislocation-prone SiC and GaN bulk crystals, called "open-core dislocations" or "dislocation micropipes".[27,28] The equilibrium morphology of dislocation-driven 1D nanostructures should be hollow NTs when the **b** is sufficiently large.[14] Fluctuations during the crystal growth may cause oscillation between solid and hollow conditions and voided NWs.

The lattice twist relationship in hollow NTs is more complex. The overall energy per unit length for a hollow nanostructure is now composed of three terms: the surface energy from the inner tube, the dislocation-induced lattice strain, and the reduction in lattice strain due to Eshelby twist:[14]

$$E = 2\pi\gamma r + \frac{\mu\mathbf{b}^2}{4\pi}\ln\left(\frac{R}{r}\right) - \frac{\mu\mathbf{b}^2}{4\pi}\frac{(R^2 - r^2)}{(R^2 + r^2)}$$

where R and r are outer and inner radius of the tube, respectively. A 1D nanoobject with an outer radius R reaches its energy minimum as $dE/dr = 0$, which relates its dimensions to the Burgers vector:

$$\mathbf{b} = \sqrt{\frac{8\pi^2\gamma r}{\mu}} \times \left(\frac{R^2 + r^2}{R^2 - r^2}\right)$$

where the first factor represents the contribution from the newly generated inner surface, and the second one is the modification due to Eshelby twist. In other words, the strain energy caused by the screw dislocations can be dissipated through forming a hollow core or producing a lattice twist around the NW/NT axis. At small **b**, formation of a thick-walled NT (small r/R) with little Eshelby twist is preferred; while at large **b**, a heavily twisted thin-walled NT (large r/R) is expected. We confirmed these predictions in the dislocation-driven ZnO NTs.[14] This theory can also explain the formation of chiral carbon NTs[29] and layer-structured inorganic NTs[25] as screw dislocation driven, for which the NT wall is very thin and the Eshelby twist (i.e., the chiral angle) is large.

Structural Characterization of Dislocation-Driven Nanomaterials

While dislocation-driven growth is general, this mechanism is underappreciated because of the practical difficulties associated with visualizing dislocations and their dynamics. In contrast to catalyst-driven mechanisms where the presence of catalyst nanoparticles is often self-evident, screw dislocations are mobile and especially unstable in small volumes.[16] Nevertheless, there are other structural characteristics associated with screw dislocations, such as

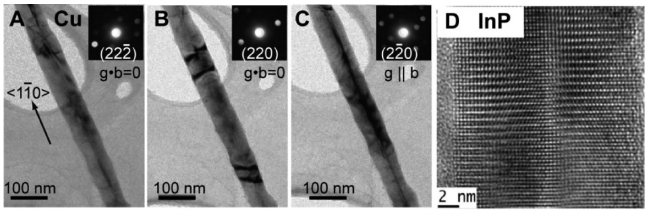

FIGURE 3. TEM imaging of screw dislocations in NWs. Panels A−C show the process of two-beam analysis on a Cu NW. (A, B) The dislocation contrast is invisible when $\mathbf{g}\cdot\mathbf{b} = 0$, and (C) the contrast is pronounced when $\mathbf{g}\|\mathbf{b}$. Panels A−C reproduced from ref 31. Copyright 2012 American Chemical Society. (D) HRTEM image of the screw dislocation in an InP NW. Reprinted with permission from ref 32. http://prl.aps.org/abstract/PRL/v107/i19/e195503 Copyright 2011 by the American Physical Society. (Readers may view, browse, and/or download material for temporary copying purposes only, provided these uses are for noncommercial personal purposes. Except as provided by law, this material may not be further reproduced, distributed, transmitted, modified, adapted, performed, displayed, published, or sold in whole or part, without prior written permission from the American Physical Society.)

Eshelby twist and hollow tubes, which can be utilized to confirm this mechanism. In this section, we introduce the common techniques to characterize dislocation-driven nanomaterials.

Diffraction Contrast of Dislocations. Transmission electron microscopy (TEM) and its associated electron diffraction techniques have been the most direct and convenient methods to analyze crystal defects. The presence of screw dislocations distorts the crystal lattice, which diffracts additional electrons and produces a dark line of contrast that can be observed by TEM. However, dislocation contrast becomes invisible when only the lattice planes corresponding to the reciprocal lattice vectors ($\mathbf{g}$) perpendicular to $\mathbf{b}$ ($\mathbf{g}\cdot\mathbf{b} = 0$) are excited during the imaging. By properly orienting a NW relative to the incident electron beam, such two-beam conditions that involve the zero beam and such $\mathbf{g}$-beams can be established; $\mathbf{b}$ is then parallel to the cross-product of the two noncollinear $\mathbf{g}$ vectors that make the dislocation invisible ($\mathbf{b}\|\mathbf{g_1}\times\mathbf{g_2}$).[30] Figure 3A−C shows the typical process of conducting the two-beam analysis to determine $\mathbf{b}$ in a Cu NW.[31] A definitive analysis requires two sets of two-beam conditions, which is sometimes difficult to achieve due to nanomaterial instability and limited tilting range of the TEM. When feasible, the direct high-resolution TEM (HRTEM) imaging of the screw dislocation shows the discontinuity of atomic planes at the dislocation core, as shown for a thin InP NW (Figure 3D).[32]

Determination of Eshelby Twist. The Eshelby twist associated with the screw dislocation is a structural characteristic that can be detected to confirm the dislocation-driven growth mechanism in 1D nanostructures. In special cases, such as branched nanotree structures (Figure 2F),[12,23,33] the twist can be directly visualized and calculated from the periodicity of the rotating branches. Occasionally, in a long or heavily twisted 1D structure, lattice rotation can result in distinct zone axes at different regions of the object. Then the twist can be determined by dividing the angle between the two zone axes with the distance, as shown in an example of a PbSe nanotree (Figure 4A).[23]

For most NWs and NTs, the twist is not always significant enough to be directly visualized but can be detected using the more sensitive twist contour analysis. Lattice twist disturbs the orientation of nonbasal planes of crystals, causing variation in electron diffraction that appears as bands/contours of contrast (Figure 4B,C). These twist contours can be analyzed using diffraction contrast TEM introduced by Drum:[34,35] the 1D object should be oriented such that a pair of $\mathbf{g}$ vectors ($\pm\mathbf{g}$) that are noncollinear with the NW/NT axial direction are excited. A zero-beam bright-field image and two dark-field images can be acquired by imposing the objective lens aperture onto each diffraction spot. A contour band can be uniquely indexed to a single $\mathbf{g}$ vector by comparing the dark-field images with the bright-field one (Figure 4C). The twist angle is then calculated as

$$\alpha = \frac{\lambda}{2L}\left|\frac{\mathbf{g}_+ - \mathbf{g}_-}{\sin\beta}\right|$$

where λ is the wavelength of the electron, L is the separation between the contour bands, and β is the angle between $\pm\mathbf{g}$ and the 1D object's axial direction. The twist contour analysis is a more sensitive technique that can quantify lattice twist less than $1^\circ/\mu$m. More importantly, it eliminates interferences from other geometric distortion, particularly the bending of the object, because bend contours can be simultaneously excited under many $\mathbf{g}$ beams.

A screw dislocation also splits the basal planes of a 1D object at its core, causing their normal to be slightly tilted relative to the growth axis. This lattice tilt can be characterized using convergent-beam electron diffraction (CBED) from which the magnitude of $\mathbf{b}$ can be calculated.[32]

Observation of Hollow NTs or Voided NWs. The template-free, spontaneous formation of single-crystal NTs is another signature of dislocation-driven growth. Such hollow structures can be conveniently visualized by TEM, because the voided regions appear brighter due to more electron transmission. We note that partially filled NTs or voided NWs should also be paid attention to, because they might be

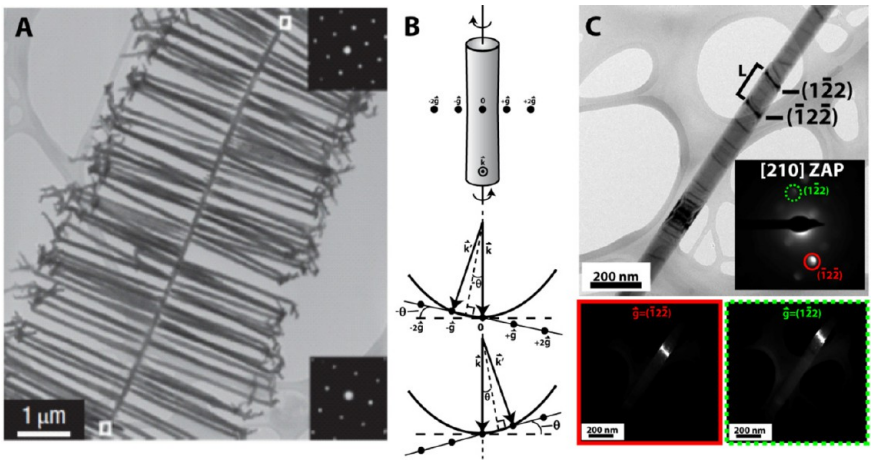

FIGURE 4. Determination of Eshelby twist. (A) Determination of lattice twist in a PbSe nanotree using selected-area electron diffraction. Reprinted from ref 23 by permission from Macmillan Publishers Ltd: [Nature Nanotechnology] (23), copyright (2008). (B) Schematic illustration of the effect of Eshelby twist on lattice diffraction. (C) Bright-field and dark-field TEM images of a twisted ZnO NW illustrating the twist contour analysis. Panels B and C reproduced from ref 34. Copyright 2010 American Chemical Society.

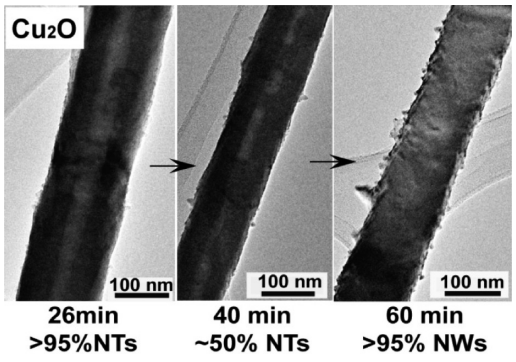

FIGURE 5. Hollow nanostructures formed by dislocation-driven growth. TEM images showing the transformation from hollow Cu_2O NTs to solid Cu_2O NWs as reaction time elapses. Reference 36 - Reproduced by permission of the Royal Society of Chemistry.

caused by gradually filling the initially empty tubes as the growth proceeds (Figure 5).[36]

Characterization of Dislocation-Driven 2D Nanoplates. The 2D nanoplates naturally prefer to lay on their basal planes when deposited onto surfaces, which displays the dislocations from the top view that are difficult to image using diffraction contrast TEM (as opposed to the side view commonly observed in NWs). On the other hand, the dislocation growth spirals are more evident from this perspective and can be directly observed using atomic force microscopy (AFM, Figure 6A) and scanning electron microscopy (SEM, Figure 6B). Moreover, 2D nanoplates can exhibit "spider contour" features in TEM images (Figure 6C), the origin of which is believed to be related to the strain field associated with screw dislocations but is yet to be understood thoroughly.[20]

General Strategies for Rational Dislocation-Driven Synthesis of Nanomaterials

The dislocation-driven NW, NT, and nanoplate growth is general and can be rationally designed. Building on the chemical vapor deposition (CVD) growth of "pine tree"-like NWs of PbS inititially discovered[12,33] and following the understanding of dislocation-driven mechanism achieved, we improved the aqueous solution growth of single-crystal ZnO NWs and NTs using flowing solutions of constant low supersaturation.[14] The generality of the dislocation-driven mechanism for different material systems and synthetic strategies (vapor or solution phase) have been demonstrated with our successful syntheses of FeOOH,[37] Cu,[31] Cu_2O,[36] and CdS/CdSe[38] NW/NTs. From these examples, we summarize the general guidelines for designing growth of anisotropic nanomaterials driven by screw dislocations. Two prerequisites should be met: (i) the presence of dislocation sources ("seeds") to initiate and propagate the growth and (ii) proper low supersaturation conditions to promote dislocation-driven growth over LBL and dendritic growth.[13] The seeding can often be achieved by introducing a spike in supersaturation at the initial stage of the reaction to create defective seed particles. We also demonstrated that the screw dislocations contained in a crystalline substrate such as GaN can be utilized to initiate NW growth.[34] This approach was also used in the electrochemical growth of Ti NWs from a metal substrate.[39] Here we focus our discussion on manipulating the growth process in order to maintain the low supersatuation. There are several strategies.

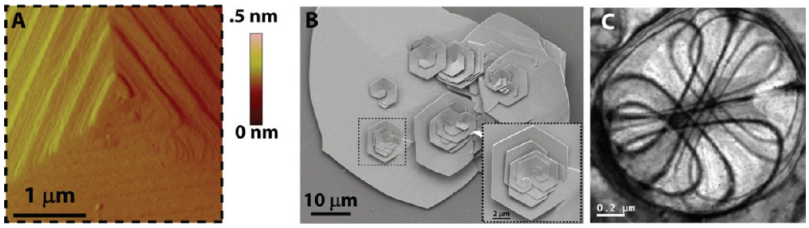

FIGURE 6. Characterization of screw dislocations in 2D zinc hydroxysulfate (ZHS) nanoplates. (A) AFM image of the dislocation core and growth spirals. (B) SEM image showing the growth spirals. (C) Spider contours observed via TEM. Reproduced from ref 20. Copyright 2011 American Chemical Society.

First, an overall low concentration or vapor pressure of reactants is preferred. For example, in the solution growth of dislocation-driven nanomaterials, the formal concentrations of the precursors are intentionally diluted, usually in micromolar to few millimolar range, and close to equilibrium.[14,36] Similarly in vapor phase syntheses, the dislocation-driven mode is promoted at lower precursor pressure, lower temperature, or both.[33,38]

Second, chemical equilibria can be coupled with the main chemical reactions responsible for forming the nanomaterial products to further modulate the supersaturation.[33] This is particularly useful in solution growth due to the versatility of solution chemistry. For instance, the concentration (supersaturation) of metal ions can be effectively controlled by adding ligands to form coordination complexes, such as in the syntheses of Cu and Cu_2O NWs.[31,36] In light of this discussion, we think the role of "surfactants" in many nanomaterial syntheses should be re-examined, since many surfactants are simultaneously effective complexation ligands that can lower the supersaturation of crystal growth. In addition, redox equilibrium[37] and other chemical equilibria[33] can also buffer the supersaturation to favor dislocation-driven growth. Essentially, all these chemical equilibria can serve as "chemical buffer systems" to maintain a low and steady supersaturation for crystal growth.

Last but not least, the maintenance of constant low supersaturation is also important to achieve steady dislocation-driven growth. In commonly practiced close-system syntheses, for example, a hydrothermal reaction, the supersaturation keeps decaying as the reaction proceeds, resulting in final morphologies convoluted by uncontrolled growth kinetics (Figure 7A). In contrast, when the reaction precursors are flowed through a reactor, as long as the feeding rate of the precursors exceeds their consumption rate, the supersaturation of the system remains constant. This is commonly practiced in CVD reactions but rarely performed for solution syntheses. We have developed a continuous flow reactor (CFR, Figure 7B)[14] to maintain constant low supersaturation level and achieve indefinite growth time and successfully applied it to the solution synthesis of ZnO,[14] FeOOH,[37] and Cu NWs.[31]

Generality of Dislocation-Driven Nanomaterial Growth

The dislocation-driven growth mechanism has been confirmed to be responsible for the growth of a variety of anisotropic nanostructures synthesized via distinct approaches in contemporary literature. Table 1 summarizes the dislocation-driven nanomaterials conclusively confirmed with experimental evidence to date, the compositions of which vary from metals, metal oxide/hydroxides, and chalcogenides to nitrides, showing the generality of the dislocation-driven mechanism. Herein we discuss representative examples to illustrate how the general guidelines in the previous section were implemented in practical syntheses.

PbS/PbSe Nanowire Trees and Other Metal Chalcogenides. The formation of the fascinating PbS/PbSe pine tree structures (Figure 2F and 4A, respectively) is the consequence of the collaboration between the dislocation-driven growth that is responsible for the trunk growth and VLS epitaxial branch overgrowth.[12,23,33] The cubic rock salt structure of PbS/PbSe is not generally known to grow anisotropically, yet the presence of dislocations breaks the symmetry of crystal growth and promotes 1D growth. We have also demonstrated the operation of dislocation-driven mechanism in the NWs of dislocation-prone wurtzite CdS/CdSe.[38] In these syntheses, the coflow of hydrogen gas was found to be crucial to promote the dislocation-driven growth. Curiously, in many vapor syntheses of nanomaterials, the introduction of H_2 usually yields more defective products, the root reason of which is not fully understood. Moreover, dislocation contrast and Eshelby twist were even observed in CdS/CdSe NWs incorporating catalyst particles. This observation suggests that the VLS and dislocation-driven growth can coexist, and it might be possible that the catalyst can induce dislocation sites to initiate the growth.

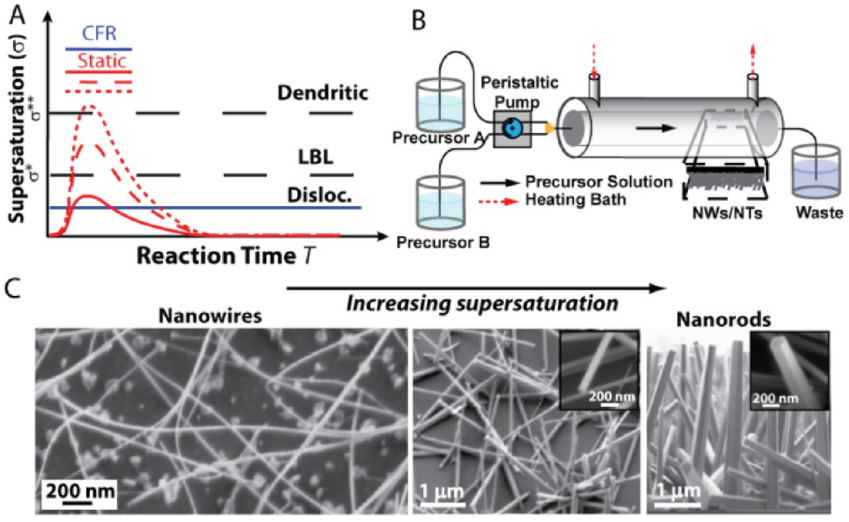

FIGURE 7. Schematics of supersaturation profiles and a general CFR design for solution synthesis of nanomaterials. (A) Schematic comparison of supersaturation profiles for static reactions and CFR reactions. (B) The CFR consists of a jacketed chromatographic column, a circulating water bath, and a peristaltic pump, enabling precise control over precursor solution composition/flow rate, reaction temperature, and reaction time. (C) Morphological change in 1D ZnO nanostructures with increasing supersaturations.[14] Adapted from ref 14. Reprinted with permission from AAAS.

TABLE 1. A Summary of Dislocation-Driven Nanomaterials Confirmed to Date

materials	morphology	synthesis	refs
PbS/PbSe	nanotree	CVD	12, 23, 33
CdS/CdSe	NW	CVD	38
InP	NW	CVD	32
AlN/GaN/InN	NW/NT	thermal nitridation	35, 46−48
In_2O_3	NW/NT	vapor deposition	49, 50
ZnO	NW/NT	hydrolysis; vapor deposition	14, 34, 41, 42
FeOOH	NW/NT	hydrolysis	37
ZHS (zinc hydroxysulfate)	nanoplate	hydrolysis	20
$Co(OH)_2$/$Ni(OH)_2$	NW/nanoplate	hydrolysis	20, 43
Cu_2O	NW/NT	solution redox	36
Cu	NW/NT	solution redox	31
Au	nanoplate	solution redox	20
Ti	NW	electrochemical deposition	39
carbon nanotubes	NT	CVD	29, 44, 45

ZnO Nanowires/Nanotubes. The solution grown ZnO NWs, NRs, and NTs via the hydrolysis of low-concentration Zn^{2+} with the presence of weak base (such as hexamethylenetetramine) as the precipitation reagent and pH buffer have been reported and utilized widely,[40] but their catalyst-free formation mechanism was not clearly understood. We have clearly confirmed that the solution growth of 1D ZnO nanostructures is driven by dislocations using TEM structural characterization and investigation of crystal growth kinetics.[14,34] We also showed that with increased supersaturation, the products' aspect ratios decrease, demonstrating the competition between dislocation-driven and LBL growth modes (Figure 7C). Observed Eshelby twist[41] or growth spirals at the tip of the NWs[42] show that ZnO NWs synthesized by vapor phase reaction can also be driven by dislocations. The commonly discussed "seeding step"[42] before many catalyst-free ZnO NW syntheses likely provides a dislocation defect-rich ZnO layer to initiate the dislocation-driven growth, similar to the function of the GaN substrate in initiating ZnO NW growth.[34]

α-FeOOH Nanowires and Other Hydroxides. α-FeOOH NWs can be grown by direct hydrolysis of Fe^{3+} ions.[37] However, Fe^{3+} ions hydrolyze quickly even at very low pH, creating difficulty in controlling the supersaturation. On the other hand, Fe^{2+} is less pH-sensitive yet prone to oxidation. Therefore, we designed the coflow of Fe^{2+} solution and Fe metal powder, where Fe^{3+} ions were generated *in situ* via the oxidation of Fe^{2+} by the dissolved O_2 and then buffered by the $Fe^{3+}/Fe^{2+}/Fe$ redox equilibria to maintain the low supersaturation that promotes the dislocation-driven growth. Using a CFR (Figure 7B) significantly increased the NW yield and aspect ratio from a static hydrothermal reaction

(Figure 8A,B). Both dislocation contrast (Figure 8C) and Eshelby twist were observed. Similarly dislocation-driven grown NWs and nanoplates of other hydroxides such as $Co(OH)_2$[20,43](Figure 8D) and $Ni(OH)_2$[20] can readily form from the direct hydrolysis of the corresponding metal salt precursors. One-dimensional nanostrustures of many other metal hydroxides or oxides, such as MnOOH, MnO_2, $In(OH)_3$, In_2O_3, SnO_2, and TiO_2, may be synthesized via a hydrolysis approach driven by screw dislocation, sometimes followed by annealing and conversion to the corresponding oxides.

Cu Nanowires/Nanotubes via Redox Reactions. Copper NWs/NTs represent a new class of materials, metal, that can be grown by screw dislocations. Their formation also involves the redox chemical reactions, which are intrinsically more complicated because the supersaturation of the reaction system is necessarily determined by both oxidizing and reducing agents. We controlled the supersaturation using low formal concentration of Cu^{2+} (oxidizing reagent) and hydrazine precursors (reducing reagent), as well as high concentrations of complexing ligands OH^- and ethylenediamine.[31] These created low and well-buffered supersaturation conditions for dislocation-driven growth of Cu. The dislocation-driven growth of Cu_2O NWs/NTs (Figure 5B) was similarly designed: low concentrations of Cu^{2+} and glucose were used as the oxidizing and reducing reagents, respectively; while OH^- and tartrate ions form stable complexes with Cu^{2+} that further lower the supersaturation.[36]

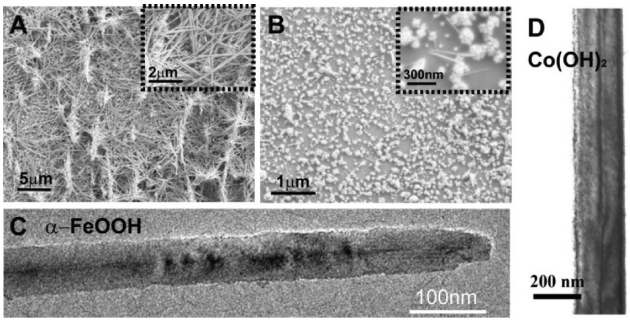

FIGURE 8. Metal hydroxide/oxyhydroxide NWs driven by dislocations. SEM images of R-FeOOH NWs from a CFR reaction (A) and a static reaction (B). TEM images showing the dislocation contrast in α-FeOOH (C) and a $Co(OH)_2$ (D) NW). Panels A to C reproduced from ref 37. Copyright 2011 American Chemical Society. Panel D adapted from ref 43. Copyright 2010 American Chemical Society.

The concept of dislocation-driven growth in redox reactions is very relevant in electrochemical deposition synthesis, where the applied overpotential is essentially the supersaturation of the system and can be easily manipulated: smaller overpotential means lower supersaturation that favors the dislocation-driven growth. The recent report of electrochemical deposition of Ti NWs initiated from dislocations in strained substrates (Figure 9F) strongly supports this argument.[39]

Single-Walled Carbon Nanotubes (SWCNTs). The general theory of dislocation-driven growth of NTs can also explain the formation and structure of SWCNTs[29,44] and

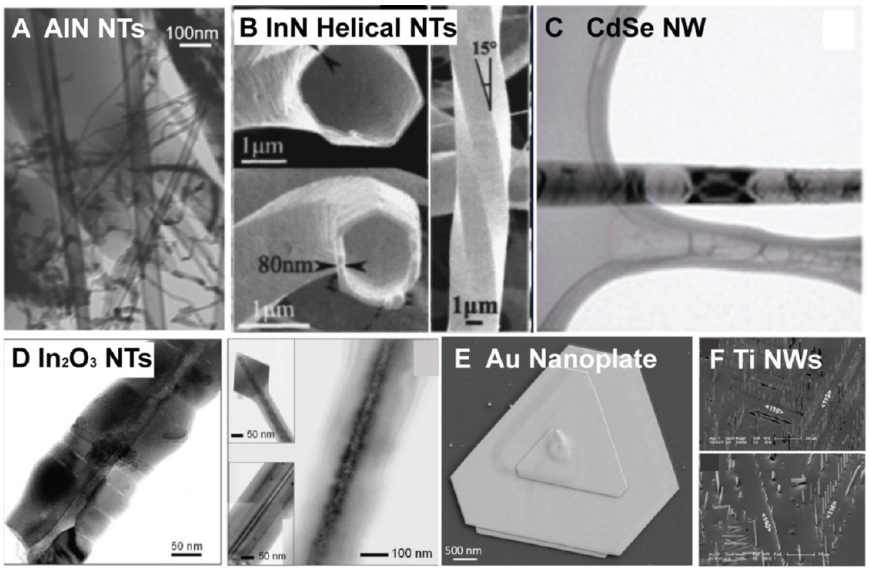

FIGURE 9. A collection of TEM or SEM images of various nanostructures driven by dislocations. Panel A adapted from ref 47. Copyright 2003 American Chemical Society. Panel B reprinted with permission from ref 48. Copyright 2005 American Institute of Physics. Panel C adapted from ref 38. Copyright 2012 American Chemical Society. Panel D adapted from ref 49 and 50. Copyright 2011 American Chemical Society. Panel E adapted from ref 20. Copyright 2011 American Chemical Society. Panel F adapted from ref 39. doi:10.1088/0957-4484/23/12/125601 © IOP Publishing. Reproduced by permission of IOP Publishing. All rights reserved.

other NTs of layered inorganic structures;[25] they are essentially NTs with extremely thin walls of single-atom or -layer thickness, and their chiral angles represent the Eshelby twist. In fact, Yakobson and co-workers suggested that the growth of chiral armchair SWCNTs can be considered as driven by axial screw dislocations and their growth rates are correlated with the magnitudes of Burgers vectors,[29] which was experimentally confirmed using *in situ* Raman spectroscopy.[45] The chirality-controlled synthesis of SWCNT has been a major challenge, and the dislocation-driven growth could provide additional ideas to address this challenge.

Other Nanostructures. Figure 9 exhibits a variety of other anisotropic nanomaterials that have been grown via dislocation-driven mechanisms. Among them, the wurtzite III-nitrides are prone to having screw dislocations. Not surprisingly, hollow structures of GaN,[46] AlN (Figure 9A),[47] and InN (Figure 9B)[48] have been reported. Especially, the thin faceted tubular structures of InN display clear Eshelby twist, which is consistent with the prediction by our model on dislocated NTs.[14] Evidence of dislocation in wurtzite CdSe NWs[38] are also shown in Figure 9C. Other examples of dislocation-driven nanostructures include In_2O_3 NTs with complex defect structures,[49,50] Au nanoplates,[20] and Ti NW arrays[39] (Figure 9D–F). Despite their distinct morphologies and reaction chemistry, these nanostructures can all be explained by the theory of dislocation-driven growth in a unified way.

Summary and Outlooks

We have shown that dislocation-driven growth is a general and versatile mechanism to synthesize a variety of anisotropic nanostructures. Distinct morphologies, from 1D to 2D to 3D, can be unified with the theory of dislocation-driven crystal growth. The microstructural characterization techniques discussed will facilitate the future search for dislocation-driven nanomaterials and confirmation of the growth mechanism. Moreover, we outlined the general framework to rationally grow nanomaterials driven by screw dislocations, which opens up the exploitation of large-scale and low-cost catalyst-free solution synthesis of anisotropic nanomaterials for diverse applications, especially nanocomposites and renewable energy applications that demand large scale. Indeed, we have recently utilized dislocation-driven growth to synthesize FeF_3 NWs from solutions and demonstrate their utility as high-capacity lithium ion battery cathodes.[51] The FeF_3 NWs can be further converted into Fe_2O_3 (hematite) NWs that show good performance in photoelectrochemical splitting of water.[52]

In the future, it would be interesting to utilize the dislocation-driven growth mechanism to grow more complicated nanostructures. Variation in the nanomorphology, complex heterostructures,[6] and more complex materials, such as ternary oxides and sulfides, are exciting and feasible targets. Because dislocation growth does not require metal catalysts, more materials can be grown into 1D nanostructures or synthesized in different ways using this versatile method. The seeding process of dislocation growth has been less studied and can be improved. For example, it could be promising to pattern the nanomaterial growth by intentionally engineering the locations of dislocation sources.[34,39] How screw dislocation spirals evolve and differentiate into different morphologies due to impurities, mass transport, size of the seeding crystals, or other factors[21] needs to be theoretically and experimentally investigated in detail, and such fundamental understanding can facilitate more rational controlled dislocation-driven nanomaterial growth. Furthermore, while there has been extensive study on the impact of dislocations on the physical properties of bulk materials,[53] it is still interesting to investigate the effect of a single screw dislocation in a single NW both theoretically and experimentally. A recent theoretical work shows that the presence of axial screw dislocation alters the bandgap of semiconducting Si and ZnO NWs,[54] suggesting a novel platform for tuning the properties of nanomaterials through defect-engineering. Deeper understanding of the dislocation-driven growth of nanomaterials and their properties and better control over such growth will add a new dimension to nanomaterial design and synthesis for various applications.

This research is supported by NSF DMR-1106184. S.J. also thanks Research Corporation SciaLog Award for Solar Energy Conversion and University of Wisconsin Vilas Associate Award for support.

BIOGRAPHICAL INFORMATION

Fei Meng (B.S. in Chemistry, Peking University, China, 2009) is currently a Ph.D. candidate at the University of Wisconsin—Madison.

Stephen A. Morin (Ph.D. in Chemistry, the University of Wisconsin—Madison, 2011) is currently a Postdoctoral Fellow at Harvard University in the laboratory of Professor George Whitesides.

Audrey Forticaux (B.S. 2009 and M.S. 2012, Ecole Superieure de Chimie, Physique et Electronique, CPE Lyon, France) is currently a Ph.D. candidate at the University of Wisconsin—Madison.

Song Jin (Ph.D. in Chemistry, Cornell University, 2002) is currently an associate professor of chemistry at the University of Wisconsin—Madison. Dr. Jin is interested in the fundamental formation mechanisms of nanomaterials, their novel physical properties, and applications in renewable energy such as solar and thermoelectric energy conversion and energy storage, nanospintronics, and nanobiotechnology.

FOOTNOTES

*Corresponding author. E-mail: jin@chem.wisc.edu.
The authors declare no competing financial interest.
‡S.A.M.: Department of Chemistry and Chemical Biology, Harvard University, 12 Oxford Street, Cambridge, Massachusetts 02138, United States.

REFERENCES

1 Xia, Y.; Yang, P.; Sun, Y.; Wu, Y.; Mayers, B.; Gates, B.; Yin, Y.; Kim, F.; Yan, H. One-Dimensional Nanostructures: Synthesis, Characterization, and Applications. *Adv. Mater.* **2003**, *15*, 353–389.

2 Yang, P.; Yan, R.; Fardy, M. Semiconductor Nanowire: What's Next? *Nano Lett.* **2010**, *10*, 1529–1536.

3 Hochbaum, A. I.; Yang, P. Semiconductor Nanowires for Energy Conversion. *Chem. Rev.* **2010**, *110*, 527–546.

4 Szczech, J. R.; Higgins, J. M.; Jin, S. Enhancement of the Thermoelectric Properties in Nanoscale and Nanostructured Materials. *J. Mater. Chem.* **2011**, *21*, 4037–4055.

5 Schmitt, A. L.; Higgins, J. M.; Szczech, J. R.; Jin, S. Synthesis and Applications of Metal Silicide Nanowires. *J. Mater. Chem.* **2010**, *20*, 223–235.

6 Bierman, M. J.; Jin, S. Potential Applications of Hierarchical Branching Nanowires in Solar Energy Conversion. *Energy Environ. Sci.* **2009**, *2*, 1050–1059.

7 Wagner, R. S.; Ellis, W. C. Vapor-Liquid-Solid Mechanism of Single Crystal Growth. *Appl. Phys. Lett.* **1964**, *4*, 89–90.

8 Morales, A. M.; Lieber, C. M. A Laser Ablation Method for the Synthesis of Crystalline Semiconductor Nanowires. *Science* **1998**, *279*, 208–211.

9 Trentler, T. J.; Hickman, K. M.; Goel, S. C.; Viano, A. M.; Gibbons, P. C.; Buhro, W. E. Solution-Liquid-Solid Growth of Crystalline III-V Semiconductors - an Analogy to Vapor-Liquid-Solid Growth. *Science* **1995**, *270*, 1791–1794.

10 Persson, A. I.; Larsson, M. W.; Stenstrom, S.; Ohlsson, B. J.; Samuelson, L.; Wallenberg, L. R. Solid-Phase Diffusion Mechanism for GaAs Nanowire Growth. *Nat. Mater.* **2004**, *3*, 677–681.

11 Sears, G. W. A Growth Mechanism for Mercury Whiskers. *Acta Metall.* **1955**, *3*, 361–366.

12 Bierman, M. J.; Lau, Y. K. A.; Kvit, A. V.; Schmitt, A. L.; Jin, S. Dislocation-Driven Nanowire Growth and Eshelby Twist. *Science* **2008**, *320*, 1060–1063.

13 Jin, S.; Bierman, M. J.; Morin, S. A. A New Twist on Nanowire Formation: Screw-Dislocation-Driven Growth of Nanowires and Nanotubes. *J. Phys. Chem. Lett.* **2010**, *1*, 1472–1480.

14 Morin, S. A.; Bierman, M. J.; Tong, J.; Jin, S. Mechanism and Kinetics of Spontaneous Nanotube Growth Driven By Screw Dislocations. *Science* **2010**, *328*, 476–480.

15 Markov, I. V. *Crystal Growth For Beginners: Fundamentals of Nucleation, Crystal Growth, and Epitaxy*, 1st ed.; World Scientific Publishing: Singapore, 1995.

16 Hirth, J. R.; Lothe, J. *Theory of Dislocations*; McGraw-Hill: New York, 1968.

17 Burton, W. K.; Cabrera, N.; Frank, F. C. Role of Dislocations in Crystal Growth. *Nature* **1949**, *163*, 398–399.

18 Burton, W. K.; Cabrera, N.; Frank, C. The Growth of Crystals and the Equilibrium Structure of Their Surfaces. *Philos. Trans. R. Soc., A* **1951**, *243*, 299–358.

19 Sunagawa, I. *Crystals: Growth, Morphology and Perfection*; Cambridge University Press: Cambridge, U.K., 2005.

20 Morin, S. A.; Forticaux, A.; Bierman, M. J.; Jin, S. Screw Dislocation-Driven Growth of Two-Dimensional Nanoplates. *Nano Lett.* **2011**, *11*, 4449–4455.

21 Doremus, R. H.; Roberts, B. W.; Turnbull, D. *Growth and Perfection of Crystals*; Wiley: New York, 1958.

22 Eshelby, J. D. Screw Dislocations in Thin Rods. *J. Appl. Phys.* **1953**, *24*, 176–179.

23 Zhu, J.; Peng, H.; Marshall, A. F.; Barnett, D. M.; Nix, W. D.; Cui, Y. Formation of Chiral Branched Nanowires by the Eshelby Twist. *Nat. Nanotechnol.* **2008**, *3*, 477–481.

24 Nikiforov, I.; Zhang, D.; Dumitrica, T. Screw Dislocations in ⟨100⟩ Silicon Nanowires: An Objective Molecular Dynamics Study. *J. Phys. Chem. Lett.* **2011**, *2*, 2544–2548.

25 Zhang, D.; Dumitrica, T.; Seifert, G. Helical Nanotube Structures of MoS_2 with Intrinsic Twisting: An Objective Molecular Dynamics Study. *Phys. Rev. Lett.* **2011**, *107*, No. 065502.

26 Zhang, D. B.; Akatyeva, E.; Dumitrica, T. Helical BN and ZnO Nanotubes with Intrinsic Twisting: An Objective Molecular Dynamics Study. *Phys Rev B* **2011**, *84*, No. 115431.

27 Frank, F. C. Capillary Equilibria of Dislocated Crystals. *Acta Crystallogr.* **1951**, *4*, 497–501.

28 Heindl, J.; Strunk, H. P.; Heydemann, V. D.; Pensl, G. Micropipes: Hollow Tubes in Silicon Carbide. *Phys. Status Solidi A* **1997**, *162*, 251–262.

29 Ding, F.; Harutyunyan, A. R.; Yakobson, B. I. Dislocation Theory of Chirality-Controlled Nanotube Growth. *Proc. Natl. Acad. Sci. U.S.A.* **2009**, *106*, 2506–2509.

30 Williams, D. B.; Carter, C. B. *Transmission Electron Microscopy: A Textbook for Materials Science*, 1st ed.; Plenum Press: New York, 1996.

31 Meng, F.; Jin, S. The Solution Growth of Copper Nanowires and Nanotubes is Driven by Screw Dislocations. *Nano Lett.* **2012**, *12*, 234–239.

32 Tizei, L. H. G.; Craven, A. J.; Zagonel, L. F.; Tencé, M.; Stéphan, O.; Chiaramonte, T.; Cotta, M. A.; Ugarte, D. Enhanced Eshelby Twist on Thin Wurtzite InP Nanowires and Measurement of Local Crystal Rotation. *Phys. Rev. Lett.* **2011**, *107*, No. 195503.

33 Lau, Y. K. A.; Chernak, D. J.; Bierman, M. J.; Jin, S. Formation of PbS Nanowire Pine Trees Driven by Screw Dislocations. *J. Am. Chem. Soc.* **2009**, *131*, 16461–16471.

34 Morin, S. A.; Jin, S. Screw Dislocation-Driven Epitaxial Solution Growth of ZnO Nanowires Seeded by Dislocations in GaN Substrates. *Nano Lett.* **2010**, *10*, 3459–3463.

35 Drum, C. M. Twist and Axial Imperfections in Filamentary Crystals of Aluminum Nitride. II. *J. Appl. Phys.* **1965**, *36*, 824–829.

36 Hacialioglu, S.; Meng, F.; Jin, S. Facile and Mild Solution Synthesis of Cu_2O Nanowires and Nanotubes Driven by Screw Dislocations. *Chem. Commun.* **2012**, *48*, 1174–1176.

37 Meng, F.; Morin, S. A.; Jin, S. Rational Solution Growth of α-FeOOH Nanowires Driven by Screw Dislocations and Their Conversion to α-Fe_2O_3 Nanowires. *J. Am. Chem. Soc.* **2011**, *133*, 8408–8411.

38 Wu, H.; Meng, F.; Li, L.; Jin, S.; Zheng, G. Dislocation-Driven CdS and CdSe Nanowire Growth. *ACS Nano* **2012**, *6*, 4461–4468.

39 Huang, X.; Chumlyakov, Y. I.; Ramirez, A. G. Defect-Driven Synthesis of Self-Assembled Single Crystal Titanium Nanowires via Electrochemistry. *Nanotechnology* **2012**, *23*, No. 125601.

40 Vayssieres, L.; Keis, K.; Lindquist, S. E.; Hagfeldt, A. Purpose-Built Anisotropic Metal Oxide Material: 3D Highly Oriented Microrod Array of ZnO. *J. Phys. Chem. B* **2001**, *105*, 3350–3352.

41 Aleman, B.; Ortega, Y.; Garcia, J. A.; Fernandez, P.; Piqueras, J. Fe Solubility, Growth Mechanism, And Luminescence of Fe Doped ZnO Nanowires and Nanorods Grown by Evaporation-Deposition. *J. Appl. Phys.* **2011**, *110*, No. 014317.

42 Park, W.; Kim, D.; Jung, S.; Yi, G. Metalorganic Vapor-Phase Epitaxial Growth of Vertically Well-Aligned ZnO Nanorods. *Appl. Phys. Lett.* **2002**, *80*, 4232–4234.

43 Li, Y.; Wu, Y. Critical Role of Screw Dislocation in the Growth of $Co(OH)_2$ Nanowires as Intermediates for Co_3O_4 Nanowire Growth. *Chem. Mater.* **2010**, *22*, 5537–5542.

44 Iijima, S. Helical Microtubules of Graphitic Carbon. *Nature* **1991**, *354*, 56–58.

45 Rao, R.; Liptak, D.; Cherukuri, T.; Yakobson, B. I.; Maruyama, B. In Situ Evidence for Chirality-Dependent Growth Rates of Individual Carbon Nanotubes. *Nat. Mater.* **2012**, *11*, 213–216.

46 Jacobs, B. W.; Crimp, M. A.; McElroy, K.; Ayres, V. M. Nanopipes in Gallium Nitride Nanowires and Rods. *Nano Lett.* **2008**, *8*, 4353–4358.

47 Wu, Q.; Hu, Z.; Wang, X.; Lu, Y.; Chen, X.; Xu, H.; Chen, Y. Synthesis and Characterization of Faceted Hexagonal Aluminum Nitride Nanotubes. *J. Am. Chem. Soc.* **2003**, *125*, 10176–10177.

48 Luo, S.; Zhou, W.; Wang, W.; Zhang, Z.; Liu, L.; Dou, X.; Wang, J.; Zhao, X.; Liu, D.; Gao, Y.; Song, L.; Xiang, Y.; Zhou, J.; Xie, S. Template-Free Synthesis of Helical Hexagonal Microtubes of Indium Nitride. *Appl. Phys. Lett.* **2005**, *87*, No. 063109.

49 Maestre, D.; Haeussler, D.; Cremades, A.; Jaeger, W.; Piqueras, J. Nanopipes in In_2O_3 Nanorods Grown by a Thermal Treatment. *Cryst. Growth Des.* **2011**, *11*, 1117–1121.

50 Maestre, D.; Haussler, D.; Cremades, A.; Jager, W.; Piqueras, J. Complex Defect Structure in the Core of Sn-Doped In_2O_3 Nanorods and Its Relationship with a Dislocation-Driven Growth Mechanism. *J. Phys. Chem. C* **2011**, *115*, 18083–18087.

51 Li, L.; Meng, F.; Jin, S. High-Capacity Lithium-Ion Battery Conversion Cathodes Based on Iron Fluoride Nanowires and Insights into the Conversion Mechanism. *Nano Lett.* **2012**, *12*, 6030–6037.

52 Li, L.; Yu, Y.; Meng, F.; Tan, Y.; Hamers, R. J.; Jin, S. Facile Solution Synthesis of α-$FeF_3 \cdot 3H_2O$ Nanowires and Their Conversion to α-Fe_2O_3 Nanowires for Photoelectrochemical Application. *Nano Lett.* **2012**, *12*, 724–731.

53 Labusch, R.; Schroeter, W. Electrical properties of dislocations in semiconductors. In *Dislocations in Solids*; Nabarro, F. R. N., Ed.; North-Holland Publishing Company: Amsterdam, 1980; Vol. 5; pp 127−191.

54 Akatyeva, E.; Kou, L.; Nikiforov, I.; Frauenheim, T.; Dumitrica, T. Electrically Active Screw Dislocations in Helical ZnO and Si Nanowires and Nanotubes. *ACS Nano* **2012**, *6*, 10042–10049.